Cell, Vol. 119, 431–443, October 29, 2004, Copyright ©2004 by Cell Press

JunB Deficiency Leads to a Myeloproliferative Disorder Arising from Hematopoietic Stem Cells

Emmanuelle Passegué,[1,*] Erwin F. Wagner,[2] and Irving L. Weissman[1]

[1]Institute of Cancer and Stem Cell Biology and Medicine
Departments of Pathology and Developmental Biology
Stanford University School of Medicine
Stanford, California 94305

[2]Research Institute of Molecular Pathology (IMP)
Dr. Bohr-Gasse 7
A-1030 Vienna
Austria

Summary

The AP-1 transcription factor JunB is a transcriptional regulator of myelopoiesis. Inactivation of JunB in postnatal mice results in a myeloproliferative disorder (MPD) resembling early human chronic myelogenous leukemia (CML). Here, we show that JunB regulates the numbers of hematopoietic stem cells (HSC). JunB overexpression decreases the frequency of long-term HSC (LT-HSC), while JunB inactivation specifically expands the numbers of LT-HSC and granulocyte/macrophage progenitors (GMP) resulting in chronic MPD. Further, we demonstrate that *jun*B inactivation must take place in LT-HSC, and not at later stages of myelopoiesis, to induce MPD and that only *jun*B-deficient LT-HSC are capable of transplanting the MPD to recipient mice. These results demonstrate a stem cell-specific role for JunB in normal and leukemic hematopoiesis and provide experimental evidence that leukemic stem cells (LSC) can reside at the LT-HSC stage of development in a mouse model of MPD.

Introduction

Hematopoiesis takes place through the stepwise differentiation of multipotent hematopoietic stem cells (HSC) (Spangrude et al., 1988) to generate a hierarchy of progenitor populations with progressively restricted developmental potential, ultimately leading to the production of multiple lineages of mature cells (Orkin, 2000). HSC can be divided into a long-term subset (LT-HSC), capable of extensive self-renewal, and a short-term subset (ST-HSC), which self-renews for a limited interval and then gives rise to non-self-renewing multipotent progenitors (MPP) (Morrison et al., 1997; Christensen and Weissman, 2001). MPP differentiate to produce both the lymphoid lineage, giving rise to common lymphoid progenitors (CLP) (Kondo et al., 1997), and the myeloid lineage, giving rise to common myeloid progenitors (CMP) (Akashi et al., 1999). CMP, in turn, differentiate into megakaryocytic/erythroid progenitors (MEP) and myelomonocytic progenitors (GMP), which finally produce mature macrophages and granulocytes (Akashi et al., 1999).

Within this developmental scheme, leukemias can now be viewed as aberrant hematopoietic processes initiated by rare leukemic stem cells (LSC) that undergo an aberrant and poorly regulated process of organogenesis analogous to that of normal HSC (Reya et al., 2001; Passegué et al., 2003). Since a hallmark of all cancers is the capacity for unlimited self-renewal, it has been proposed, although never directly demonstrated, that leukemias may be initiated by transforming events that directly take place in the self-renewing LT-HSC. Alternatively, leukemias may also arise from more committed progenitors that have re-acquired the capacity for indefinite self-renewing proliferation through accumulated mutations and/or epigenetic changes, as we have recently shown for some human acute myeloid leukemia (AML) (Miyamoto et al., 2000) and late-stage human chronic myelogenous leukemia (CML) (Jamieson et al., 2004). Identifying the developmental origin of the LSC for each type of leukemia is therefore critical for understanding their respective biology and providing powerful diagnostic, prognostic, and therapeutic tools in the clinic.

At the molecular level, the mechanisms controlling HSC self-renewal activity are still poorly understood. However, the signaling pathways that have been shown to date to be involved in the regulation of HSC self-renewal, i.e., homeobox genes, such as *HoxB4* (Antonchuk et al., 2002) and *HoxA9* (Thorsteinsdottir et al., 2002), *Notch* (Varnum-Finney et al., 2000), *Sonic hedgehog* (*Shh*) (Bhardwaj et al., 2001), the *Wnt* signaling pathway (Reya et al., 2003), and *Bmi-1* (Park et al., 2003; Lessard and Sauvageau, 2003), have also been associated with oncogenesis and/or overt leukemia (Reya et al., 2001; Lessard and Sauvageau, 2003), suggesting the intriguing hypothesis that similar molecular mechanisms may control self-renewal activity in normal hematopoietic stem cells and malignant stem cells.

The AP-1 transcription factor JunB is a transcriptional regulator of myelopoiesis and a potential tumor suppressor gene in mice (Passegué et al., 2001). Inactivation of *jun*B in knockout mice results in severe vascular defects in the placenta leading to early embryonic lethality, while constitutive overexpression of *jun*B from the human ubiquitin-C promoter (Ubi) has no major consequences in Ubi-*jun*B transgenic mice (Schorpp-Kistner et al., 1999). Reintroducing *jun*B expression in the *jun*B-deficient background by intercrossing with Ubi-*jun*B transgenic mice fully rescues the mice from embryonic lethality (Schorpp-Kistner et al., 1999). However, all resulting *jun*B$^{-/-}$Ubi-*jun*B mice progressively develop a transplantable myeloproliferative disorder (MPD) with some features of human CML, including eventual progression to blast crisis associated with an age-dependent and what was originally described to be myeloid-specific silencing of the Ubi-*jun*B transgene (Passegué et al., 2001). Remarkably, inactivation of *jun*B expression is also observed in some human CML patients (Bruchova et al., 2002; Yang et al., 2003), and downregulation

*Correspondence: passegue@stanford.edu

of *jun*B expression is consistently found in AML patients expressing high levels of HoxA9 (Dorsam et al., 2003). Together, these findings suggest that *jun*B inactivation could be important for MPD development and perhaps overt myeloid leukemia including CML.

Here, we use the *jun*B$^{-/-}$Ubi-*jun*B model, as well as several novel models of conditional inactivation and overexpression of *jun*B in hematopoietic cells, to investigate the function of JunB during normal and leukemic hematopoiesis. We find that loss of *jun*B expression leads to MPD development only when occurring at the stem cell level and that the LT-HSC is the sole developmental stage containing the LSC for the *jun*B-deficient MPD. Moreover, we identify JunB as a key negative regulator of LT-HSC function, controlling the numbers of LT-HSC by regulating several cellular mechanisms that are critical for maintenance of the stem cell compartment, i.e., proliferation/senescence and apoptosis, via changes in the expression levels of crucial effector genes, including the cell cycle regulators p16^{INK4a} and the antiapoptotic proteins Bcl_2 and Bcl_{xl}.

Results

Enforced Expression of JunB in LT-HSC Causes Stem Cell Loss

To test the role for JunB during normal hematopoiesis, we analyzed the consequences of enforced expression of JunB in stem cells (Figure 1). Highly purified populations of LT-HSC (Lin$^-$/c-Kit$^+$/Sca-1$^+$/Thy1.1^{int}) (Morrison et al., 1997) were isolated from C57BL/6-Ly5.2 mice, transduced with *jun*B-containing [*jun*B(L)] or control [Co(L)] lentiviruses, and transplanted into lethally irradiated C57BL/6-Ly5.1 congenic recipients (Figure 1A). Both lentiviruses infected LT-HSC with similar efficiency (37% to 45% transduction efficiency), and FACS analysis of peripheral blood isolated from recipient mice at 3 weeks post-transplantation revealed similar engraftment and short-term multilineage reconstitution (Figure 1B; data not shown). However, over time, a dramatic decline in the numbers of transduced Ly5.2$^+$/GFP$^+$ cells was observed in the blood of mice transplanted with *jun*B(L)-transduced HSC compared to the fairly constant level found in the blood of mice transplanted with Co(L)-transduced HSC. At 9 weeks post-transplantation, we used quantitative real-time RT-PCR (qRT-PCR) analysis of HSC-derived Ly5.2$^+$/GFP$^+$ spleen cells to assay the increase in *jun*B levels provided by the lentiviral transduction (Figure 1C). At 20 weeks post-transplantation, we determined the distribution of transduced Ly5.2$^+$/GFP$^+$ cells in the stem, progenitor, and mature compartments of recipient mice (Figures 1D–1F). Although transduction with the *jun*B(L) lentivirus resulted in a modest 1.8-fold increase in total *jun*B mRNA levels, dramatically reduced numbers of HSC-derived Ly5.2$^+$/GFP$^+$ cells were found in the bone marrow, spleen, and thymus of the transplanted mice. Furthermore, in the bone marrow, almost no *jun*B(L)-transduced Ly5.2$^+$/GFP$^+$ cells with the phenotypic characteristics of LT-HSC (Lin$^-$/c-Kit$^+$/Sca-1$^+$/Flk2$^-$) (Christensen and Weissman, 2001), myeloid progenitors (Lin$^-$/c-Kit$^+$/Sca-1$^-$/CD34/FcγR) (Akashi et al., 1999), or lymphoid progenitors (Lin$^-$/Il-7R$^+$/Thy1.1$^-$/c-Kit^{int}/Sca-1^{int}) (Kondo et al., 1997) could be detected, and all lineages of mature cells were dramatically reduced in number. Together, these results indicate that raising JunB levels in LT-HSC decreases the frequency of stem cells.

Increased Frequency of LT-HSC and GMP in *jun*B$^{-/-}$Ubi-*jun*B Mice

To determine the stages of hematopoietic development that are affected in the *jun*B$^{-/-}$Ubi-*jun*B model of MPD, we next examined the frequency and fate of stem cell and myeloid progenitor populations using 6- to 9-month-old *jun*B$^{-/-}$Ubi-*jun*B mice (Figure 2). The *jun*B$^{-/-}$Ubi-*jun*B mice develop by 3 to 6 months of age an MPD characterized by a massive granulocytic expansion in the bone marrow and spleen (Figures 2A and 2B), eventually followed by the appearance of undifferentiated blast cells leading to a myeloid blast crisis in 16% of the mice (Passegué et al., 2001). Initial analysis of *jun*B$^{-/-}$Ubi-*jun*B bone marrow revealed a considerable increase in HSC-enriched (Lin$^-$/c-Kit$^+$/Sca-1$^+$) and myeloid progenitor-enriched (Lin$^-$/c-Kit$^+$/Sca-1$^-$) populations (Figure 2A). Further investigation indicated that the increase in multipotent bone marrow cells resulted exclusively from an increase in the numbers of LT-HSC (Lin$^-$/c-Kit$^+$/Sca-1$^+$/Flk-2$^-$), while the numbers of ST-HSC and MPP remained similar to those found in control mice. In the myeloid lineage, only the GMP population (Lin$^-$/c-Kit$^+$/Sca-1$^-$/CD34$^+$/FcγR$^+$) displayed a massive expansion, which accounted almost entirely for the increased numbers of myeloid progenitors found in *jun*B$^{-/-}$Ubi-*jun*B mice, while the numbers of CMP and MEP remained very similar to control animals (Figure 1A). Abnormally high numbers of cells with the phenotypic characteristics of LT-HSC and GMP were also observed in the enlarged spleens of *jun*B$^{-/-}$Ubi-*jun*B mice (Figure 2B).

Stochastic Inactivation of JunB in *jun*B$^{-/-}$Ubi-*jun*B LT-HSC

To correlate the specific expansion of the LT-HSC and GMP populations with *jun*B expression, we investigated by qRT-PCR the expression profile of the Ubi-*jun*B transgene within the hematopoietic system of both Ubi-*jun*B transgenic mice and *jun*B$^{-/-}$Ubi-*jun*B MPD mice (Figure 2C). QRT-PCR revealed high expression levels of the Ubi-*jun*B transgene among the pool of multipotent bone marrow cells (LT-HSC, ST-HSC, and MPP) isolated from Ubi-*jun*B transgenic mice, with considerably lower levels in the myeloid progenitor populations (CMP, GMP, and MEP) and B cells, and no expression in mature granulocytes. Strikingly, a similar analysis performed on populations isolated from 6- to 9-month-old *jun*B$^{-/-}$Ubi-*jun*B mice showed dramatically reduced expression levels of the Ubi-*jun*B transgene in every cell type, including LT-HSC, and, consequently, a major reduction in total *jun*B mRNA levels in the entire hematopoietic system of the *jun*B$^{-/-}$Ubi-*jun*B mice (Figure 2C). Inactivation of the Ubi-*jun*B transgene in the myeloid lineage of *jun*B$^{-/-}$Ubi-*jun*B mice has been described previously (Passegué et al., 2001). However, these results indicate that transgene inactivation occurs already in the stem cell compartment, consistent with the hypothesis that clones of LT-HSC that inactivate *jun*B expression have a competitive advantage over LT-HSC that still express the Ubi-*jun*B

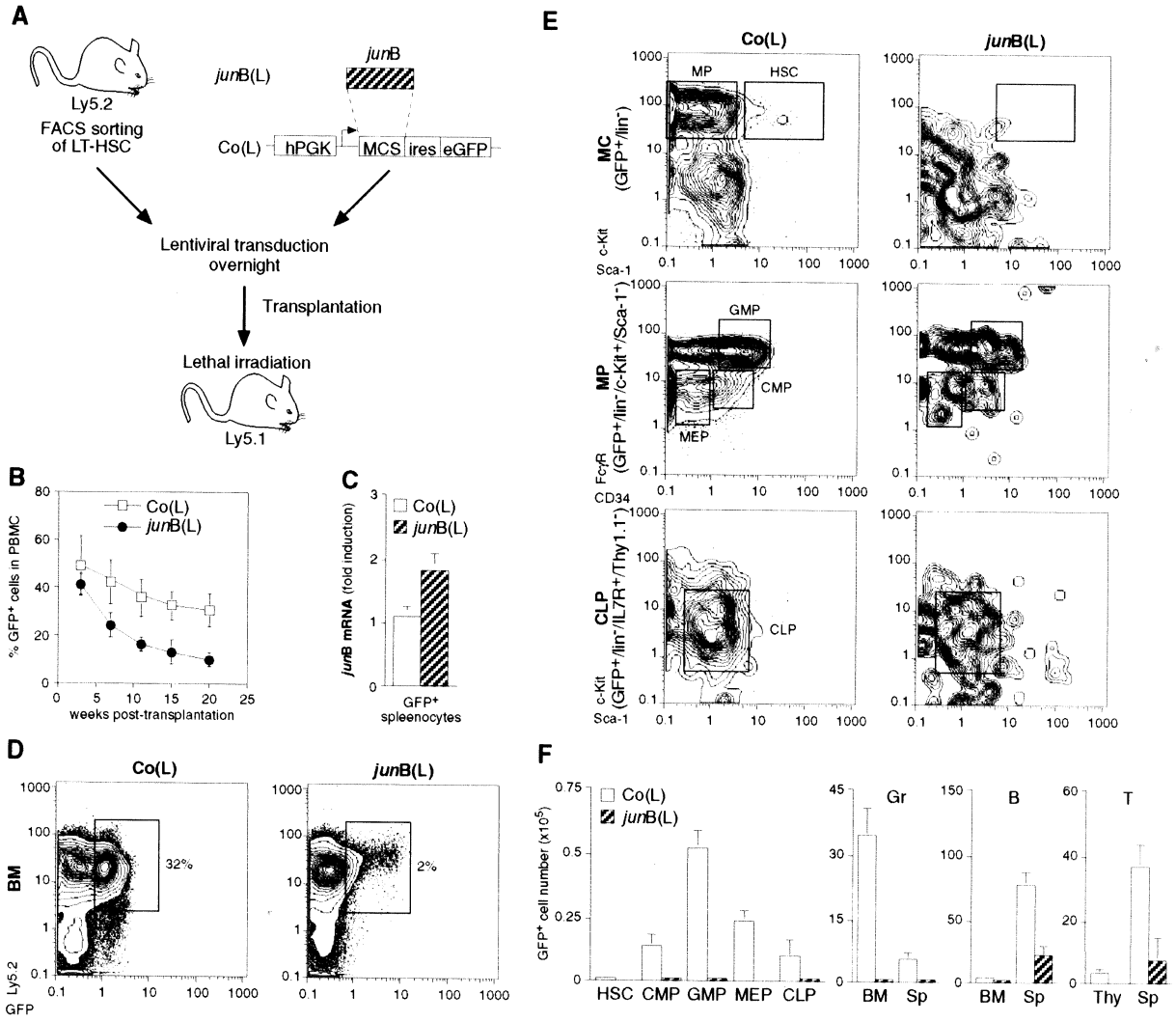

Figure 1. Enforced Expression of *junB* in LT-HSC Causes Stem Cell Loss

(A) Schematic representation of the lentiviral transduction/transplantation protocol. LT-HSC were purified from C57BL/6-Ly5.2 mice, infected overnight with an empty control [Co(L)] or a *junB*-expressing [*junB*(L)] lentivirus and transplanted into lethally irradiated C57BL/6-Ly5.1 congenic recipient mice (2,000 transduced-HSC/mouse). hPGK: human PGK promoter; MCS: multiple cloning site; ires: internal ribosomal entry site; eGFP: enhanced green fluorescent protein.

(B) Peripheral blood chimerism in mice transplanted with *junB*(L)- or Co(L)-transduced HSC. Data are plotted as percent (mean ± SD; n = 5) of GFP^+ cells in peripheral blood mononuclear cells (PBMC).

(C) QRT-PCR analysis of *junB* mRNA levels in transduced HSC-derived ($Ly5.2^+/GFP^+$) spleenocytes at 9 weeks post-transplantation. Results have been standardized for β-actin levels and are expressed as fold-induction (mean ± SD; n = 3) compared to the levels detected in Co(L)-transduced cells (set to 1).

(D–F) Flow cytometric analysis of Co(L)- and *junB*(L)-transduced HSC-derived ($Ly5.2^+/GFP^+$) cells at 20 weeks post-transplantation. (D) Overall percentage in the bone marrow. (E) Distribution in the multipotent cell (MC: Lin^-/c-Kit/Sca-1), myeloid progenitor (MP: Lin^-/c-Kit^+/Sca-1^-/CD34/FcγR), and lymphoid progenitor (CLP: Lin^-/IL7R^+/Thy1.1^-/c-Kit/Sca-1) populations. (F) Distribution in the indicated hematopoietic lineages in the bone marrow (BM), spleen (Sp), and thymus (Thy). Bar graphs indicate the total cell number (mean ± SD; n = 3) per four long bones or per spleen for each of the indicated populations. Gr: Gr-1^+/Mac-1^+; B: B220$^+$/CD19$^+$; T: CD4$^+$. Mice transplanted with *junB*(L)-transduced HSC displayed on average 20%–50% decrease in total cellularity in both bone marrow and spleen compared to mice transplanted with Co(L)-transduced HSC (not shown).

transgene, such that *junB*-deficient LT-HSC and their progeny progressively take over hematopoiesis in *junB*$^{-/-}$Ubi-*junB* mice.

Targeted Inactivation of JunB during Myelopoiesis Does Not Cause MPD

To identify directly the developmental stage where inactivation of *junB* expression is required for MPD development, we crossed mice carrying a floxed allele of *junB* (*junB*^{f}) (Kenner et al., 2004) with a granulocyte lineage-specific MRP8-*Cre*-ires/GFP transgenic mouse (Figure 3). The human MRP8 promoter restricts CRE recombinase activity, as well as expression of the GFP marker, to granulocytes and a fraction of GMP (10%–20%) (Figures 3A and 3B) (Lagasse and Weissman, 1994). Consistent with this expression pattern, specific deletion of the

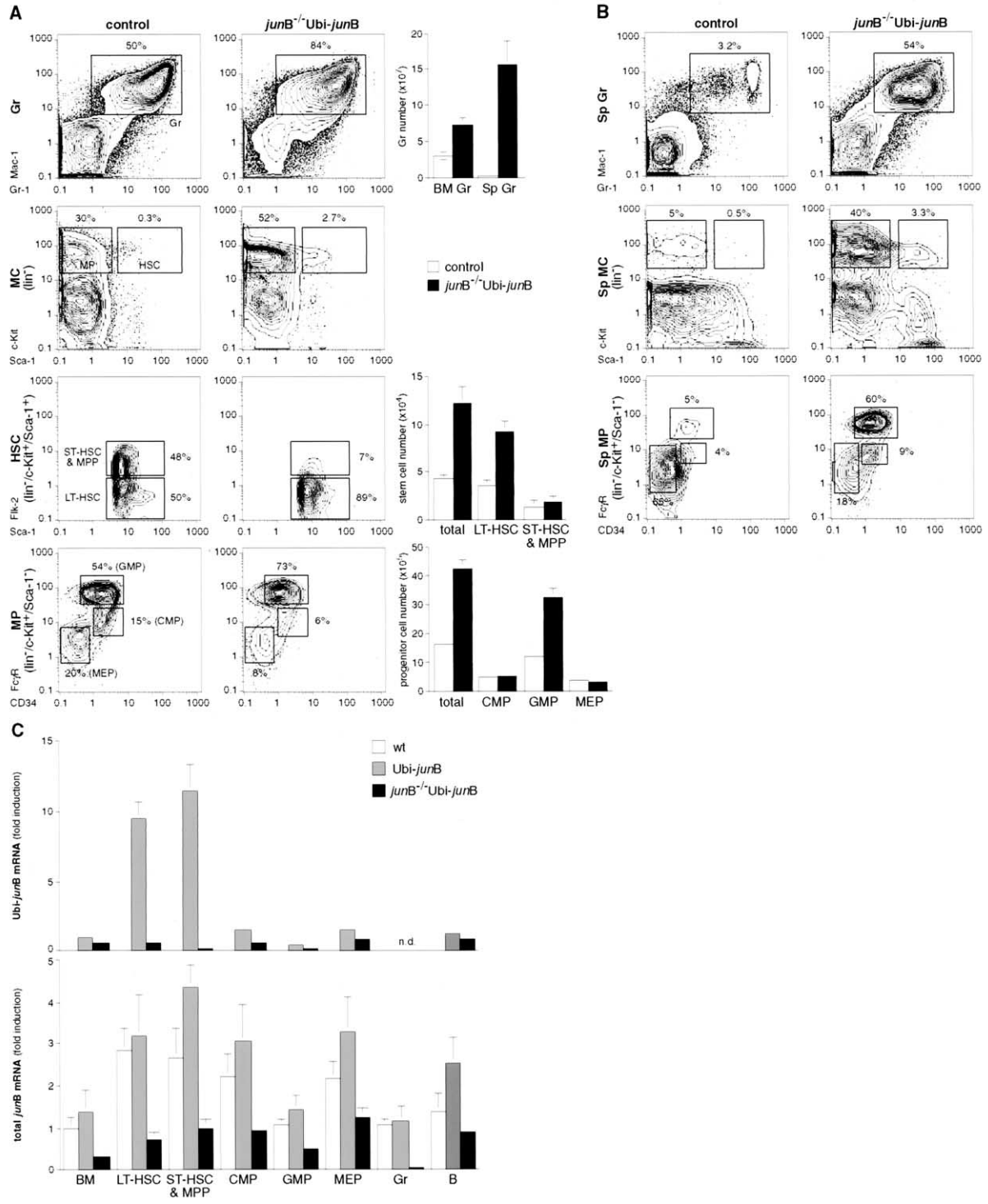

Figure 2. Specific Expansion of the LT-HSC and GMP Populations in *jun*B-Deficient *jun*B$^{-/-}$Ubi-*jun*B MPD Mice

Analysis of 6- to 9-month-old control (*jun*B$^{+/+}$ or *jun*B$^{+/-}$ with or without the Ubi-*jun*B transgene) and *jun*B$^{-/-}$Ubi-*jun*B mice.

(A and B) Detailed FACS analysis of the granulocytic (Gr: Gr-1^{+}/Mac-1^{+}), multipotent cell (MC: Lin^{-}/c-Kit/Sca-1), stem cell (HSC: Lin^{-}/c-Kit^{+}/Sca-1^{+}/Flk-2), and myeloid progenitor (MP: Lin^{-}/c-Kit^{+}/Sca-1^{-}/CD34/FcγR) populations in the bone marrow (BM) and spleen (Sp). Bar graphs indicate the total cell number (mean ± SD; n = 3) per four long bones or per spleen for each of the indicated populations. By 6 months of age, the *jun*B$^{-/-}$Ubi-*jun*B mice display on average a 1.4-fold increase in total cellularity in the bone marrow and a 2.7-fold increase in the spleen compared to control mice (not shown).

(C) QRT-PCR analysis of Ubi-*jun*B transgene (upper panel) and total *jun*B (bottom panel) mRNA levels in wild-type (wt; n = 3), Ubi-*jun*B transgenic (n = 2), and *jun*B$^{-/-}$Ubi-*jun*B (n = 3) bone marrow. Results are given as mean (±SD) of independently sorted sets of stem, progenitor, and mature cell populations. Each value has been standardized for β-actin expression level and is expressed as fold induction compared to Ubi-*jun*B levels in unfractionated transgenic bone marrow (set to 1; top panel) or to *jun*B levels in unfractionated wild-type bone marrow (set to 1; bottom panel). B: B220^{+}/CD19^{+} spleenocytes; n.d.: not detected.

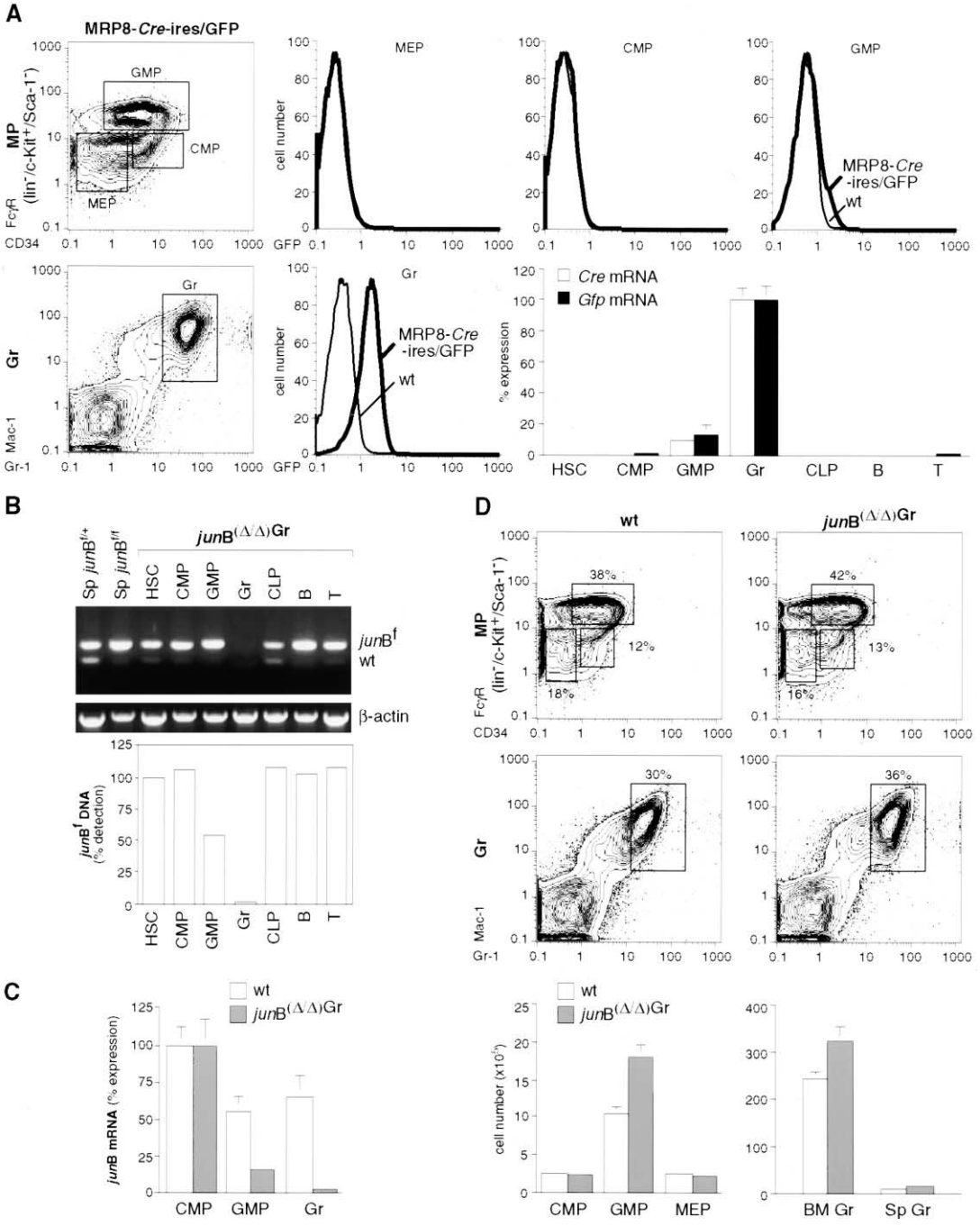

Figure 3. Myeloid-Restricted Deletion of *junB* Does Not Lead to MPD

(A and B) Characterization of MRP8-*Cre*-ires/GFP transgenic mice. (A) FACS analysis of GFP expression in myeloid progenitor (MP: Lin^-/c-Kit^+/$Sca\text{-}1^-$/CD34/FcγR) and granulocytic (Gr: Gr-1^+/Mac-1^+) populations in the bone marrow (BM). (B) QRT-PCR analysis of *Cre* and *Gfp* mRNA levels. Results (mean ± SD; n = 3) have been standardized for β-actin expression levels and are expressed as a percentage of the maximal expression levels detected in granulocytes (set to 100%). HSC: Lin^-/c-Kit^+/$Sca\text{-}1^+$ bone marrow cells; B: $B220^+$/$CD19^+$ spleenocytes; T: $CD4^+$ spleenocytes.

(C–E) Analysis of *junB*$^{f/f}$MRP8-*Cre*-ires/GFP (*junB*$^{(\Delta/\Delta)Gr}$) mice. (C) PCR analysis (upper panel) of wild-type (wt or *junB*$^+$) and floxed *junB* (*junB*^{f}) alleles in genomic DNA extracted from each of the indicated populations. Genomic DNA from spleenocytes (Sp) of the indicated genotypes were used as control. Real-time PCR quantification (lower panel) of the efficiency of deletion of the floxed *junB* alleles in the same genomic DNA. Results have been standardized for β-actin DNA levels and are expressed as percentages of the levels detected in HSC (set to 100%). (D) QRT-PCR analysis of *junB* mRNA levels in the myeloid lineage of wild-type and *junB*$^{(\Delta/\Delta)Gr}$ mice. Results (mean ± SD; n = 3) have been standardized for β-actin levels and are expressed as percentages of the levels detected in control CMP (set to 100%). (E) Detailed FACS analysis of the myeloid progenitor (MP) and granulocytic (Gr) populations in *junB*$^{(\Delta/\Delta)Gr}$ bone marrow. Bar graphs indicate the total cell number (mean ± SD; n = 3) per four long bones or per spleen for each of the indicated populations.

floxed *jun*B allele was observed in a subset of the GMP and in most, if not all, granulocytes of the *jun*B$^{f/f}$MRP8-*Cre*-ires/GFP (*jun*B$^{(\Delta/\Delta)Gr}$) mice (Figure 3C), correlating with reduced levels of *jun*B mRNA in GMP and no detectable expression in granulocytes (Figure 3D). Increased numbers of GMP and granulocytes were observed in the bone marrow of *jun*B$^{(\Delta/\Delta)Gr}$ mice, but no significant expansion of the granulocytic population was observed in the spleen (Figure 3E). Furthermore, none of the *jun*B$^{(\Delta/\Delta)Gr}$ mice (n = 18) analyzed over an observation period of 12 months showed evolution of this indolent expansion of the granulocytic lineage to blast crisis, MPD, or overt leukemia. Therefore, targeted inactivation of *jun*B in non-self-renewing myeloid progenitors is not sufficient for MPD development.

Targeted Inactivation of JunB in LT-HSC Results in MPD

We next crossed the floxed *jun*B mice with two different transgenic mice that can induce CRE expression in stem cells (Figure 4): the constitutive MORE-*Cre* knockin mice (Tallquist and Soriano, 2000) and the inducible Mx-*Cre* mice (Kühn et al., 1995). The MORE-*Cre* allele restricts the CRE recombinase activity to the embryo proper, thereby allowing the birth of *jun*B$^{f/f}$MORE-*Cre* (*jun*B$^{\Delta/\Delta}$) mice (Figure 4A), which develop several pathologies, including a severe osteoporosis by 4 weeks of age (Kenner et al., 2004) and, by 3 to 6 months, an MPD with massive granulocytic expansion in bone marrow and spleen (Figure 4D; Supplemental Figure S1A at http://www.cell.com/cgi/content/full/119/3/431/DC1/). Three-month-old *jun*B$^{\Delta/\Delta}$ mice showed undetectable levels of the floxed *jun*B allele in LT-HSC, correlating with a complete absence of *jun*B mRNA expression (Figures 4B and 4C), and, similarly to the *jun*B$^{-/-}$Ubi-*jun*B mice, displayed a massive and specific expansion of the LT-HSC and GMP populations (Figure 4D). To further study the correlation between stem cell deletion of *jun*B and MPD development in adult mice, we also used inducible Mx-*Cre* transgenic mice that, upon injection of the interferon α inducer poly(I/C), induces CRE recombinase activity in numerous cell types including stem cells in *jun*B$^{f/f}$ Mx-*cre* [*jun*B$^{(\Delta/\Delta)i}$] mice (Figure 4E). Two months after poly(I/C) injection, we confirmed complete deletion of the floxed *jun*B allele in LT-HSC (Figure 4F) and complete loss of *jun*B mRNA expression in LT-HSC (Figure 4G). Following sustained inactivation of *jun*B, all *jun*B$^{(\Delta/\Delta)i}$ mice displayed a progressive and specific expansion of the LT-HSC and GMP populations, which led by 6-9 months post-poly(I/C) injection to the development of an MPD with massive granulocytic expansion in bone marrow and spleen (Figure 4H; Supplemental Figures S1B and S1C on the *Cell* website). Together, these results indicate that inactivation of *jun*B in hematopoietic stem cells is absolutely required for MPD development. They also suggest that *jun*B-deficient HSC and GMP are qualitatively different in their ability to promote leukemogenesis.

The *jun*B-Deficient MPD Is an HSC Leukemic Disorder

To identify the developmental stage that contains the LSC for the *jun*B-deficient MPD, we first transplanted highly purified subpopulations isolated from 6- to 9-month-old *jun*B$^{-/-}$Ubi-*jun*B mice in sublethally irradiated immunocompromised *RAG2*-deficient congenic recipient mice (Table 1; Supplemental Figure S2 online). While unfractionated bone marrow always transferred the MPD in secondary recipient mice, c-Kit-depleted bone marrow did not, suggesting that the LSC resides in the stem or myeloid progenitor pools. However, neither the CMP nor the GMP populations transplanted the MPD or persisted in the primary recipient mice for longer than 6 weeks, similar to transplantation of wild-type progenitor populations (Akashi et al., 1999; Na Nakorn et al., 2002). Furthermore, CMP and GMP isolated from *jun*B$^{-/-}$Ubi-*jun*B mice displayed normal clonogenic progenitor activity in vitro, with 80%–90% of the cells plated giving rise to colonies. Transplantation of high numbers of (Lin$^-$/c-Kit$^+$/Sca-1$^-$) bone marrow cells containing a mixture of CMP, GMP, and MEP also failed to repopulate or transplant the MPD to recipient mice (Table 1), thereby excluding the possibility of a higher cell number requirement. Within the pool of multipotent bone marrow cells, only transplantation of LT-HSC resulted in the propagation of the MPD, while transplantation of the immediate next developmental stages, ST-HSC and MPP, did not (Table 1). Strikingly, as few as 60 LT-HSC were sufficient to transfer the disease to secondary recipients (data not shown). The MPD that developed in the LT-HSC-transplanted recipient mice closely mimicked the disease occurring in primary donor mice, with increased LT-HSC and GMP populations and eventual emergence of undifferentiated blast cells (Supplemental Figure S3 online). Transplantation of *jun*B$^{-/-}$Ubi-*jun*B spleen cells, which contain high numbers of cells with the phenotypic characteristics of LT-HSC, also transplanted the MPD in primary recipient mice (Table 1). Similar results were obtained using lethally irradiated nonimmunocompromised congenic recipient mice, although this model resulted in longer intervals for MPD development following transplantation of unfractionated bone marrow or purified LT-HSC (data not shown), possibly implicating a role for immunosurveillance in this disease. Finally, transplantation experiments were also performed with highly purified LT-HSC and a mixture of CMP, GMP, and MEP (Lin$^-$/c-Kit$^+$/Sca-1$^-$) isolated from 3-month-old *jun*B$^{\Delta/\Delta}$ mice or from *jun*B$^{(\Delta/\Delta)i}$ mice 4 months after poly(I/C) injection (Table 1). Similarly to the *jun*B$^{-/-}$Ubi-*jun*B mice, using these two genetically defined mouse models, we found that only transplantation of unfractionated bone marrow or purified LT-HSC was capable of propagating the MPD to recipient mice. Together, these results clearly demonstrate that the LSC are contained within the LT-HSC population, thereby establishing that the *jun*B-deficient MPD is a hematopoietic stem cell leukemia.

JunB Regulates LT-HSC Numbers through Changes in Proliferation and Apoptosis

Finally, we analyzed *jun*B-deficient LT-HSC and *jun*B(L)-expressing LT-HSC to identify cellular and molecular mechanisms that are affected by the loss or gain of *jun*B expression and are critical for maintenance of the stem cell compartment (Figure 5). Cell cycle analysis using Hoechst-33342 showed similar percentages of G_0-G_1

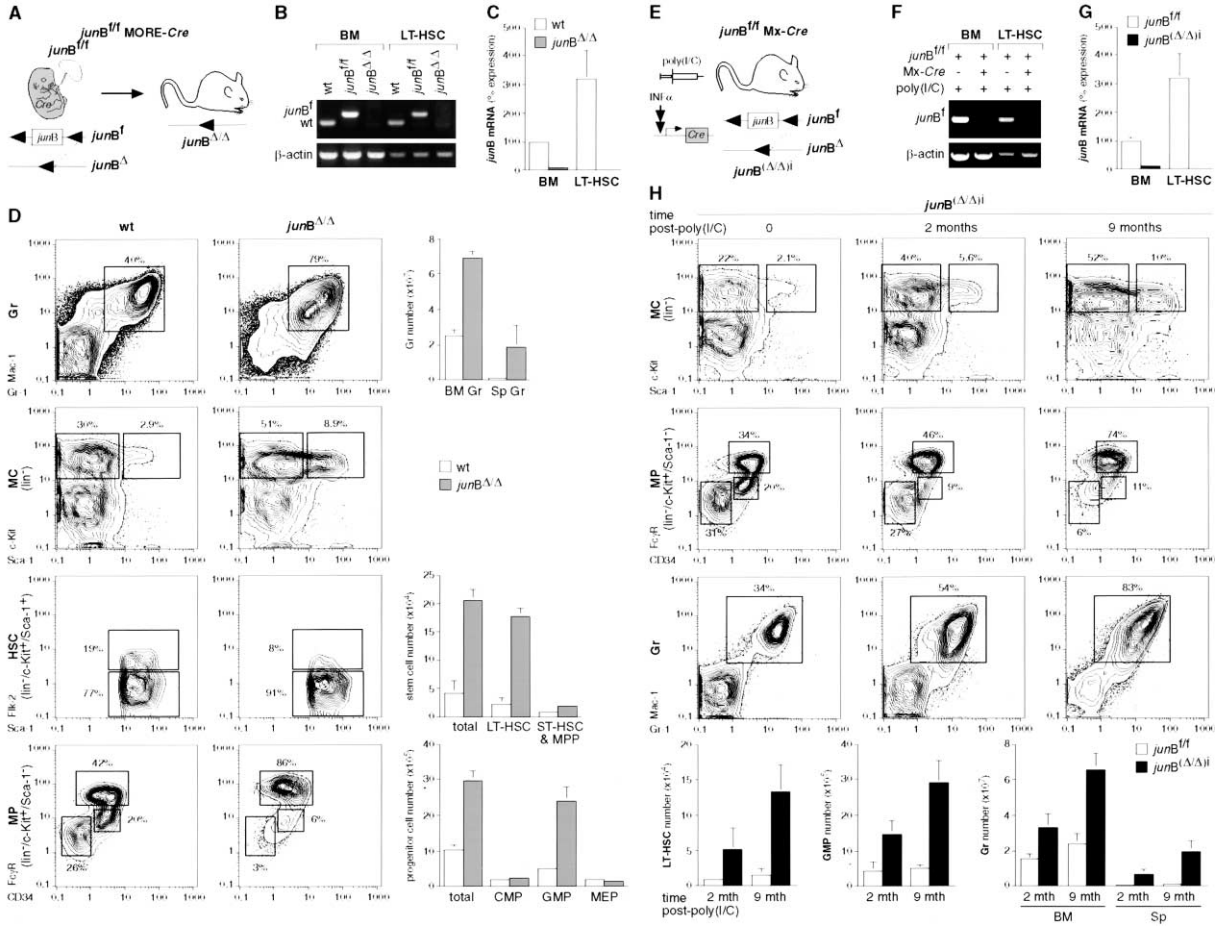

Figure 4. Stem Cell Deletion of *jun*B Leads to MPD

(A) Schematic representation of the MORE-*Cre*-mediated deletion of the floxed *jun*B alleles during embryonic development. The MORE promoter restricts CRE expression to the embryo proper and allows the birth of *junB*$^{f/f}$MORE-*Cre* (*junB*$^{\Delta/\Delta}$) mice, which are *jun*B deficient in every cell type.

(B–D) Analysis of 3-month-old *junB*$^{\Delta/\Delta}$ mice. (B) PCR analysis of wild-type (wt) and floxed *jun*B (*junB*^{f}) alleles in genomic DNA extracted from bone marrow (BM) or LT-HSC purified from mice of the indicated genotype. (C) QRT-PCR analysis *jun*B mRNA expression in bone marrow and LT-HSC purified from wild-type and *junB*$^{\Delta/\Delta}$ mice. Results (mean ± SD; n = 3) have been standardized for β-actin levels and are expressed as percentages of the levels detected in wild-type bone marrow (set to 100%). (D) Detailed FACS analysis of the granulocytic (Gr: Gr-1^{+}/Mac-1^{+}), multipotent cell (MC: Lin^{-}/c-Kit/Sca-1), stem cell (HSC: Lin^{-}/c-Kit^{+}/Sca-1^{+}/Flk-2), and myeloid progenitor (MP: Lin^{-}/c-Kit^{+}/Sca-1^{-}/CD34/FcγR) populations in *junB*$^{\Delta/\Delta}$ bone marrow. Bar graphs indicate the total cell number (mean ± SD; n = 3) per four long bones or per spleen (Sp) for each of the indicated populations. *Jun*B$^{\Delta/\Delta}$ mice display on average a 1.6-fold increase in total cellularity in the bone marrow and a 1.3-fold increase in the spleen compared to wild-type mice (not shown).

(E) Schematic representation of the Mx-*Cre*-mediated deletion of the floxed *jun*B alleles following poly(I/C) injection in *junB*$^{f/f}$Mx-*Cre* (*junB*$^{(\Delta/\Delta)i}$) mice.

(F–H) Analysis of *junB*$^{(\Delta/\Delta)i}$ mice. (F) PCR analysis of floxed *jun*B allele in genomic DNA extracted from bone marrow or LT-HSC purified from mice of the indicated genotypes at 2 months post-poly(I/C) injection. (G) QRT-PCR analysis of *jun*B mRNA expression in bone marrow and LT-HSC purified from *junB*$^{f/f}$ and *junB*$^{(\Delta/\Delta)i}$ mice at 2 months post-poly(I/C) injection. Results (mean ± SD; n = 3) have been standardized for β-actin levels and are expressed as percentages of the levels detected in *junB*$^{f/f}$ bone marrow (set to 100%). (H) Detailed FACS analysis of the multipotent cell (MC), myeloid progenitor (MP), and granulocytic (Gr) populations in *junB*$^{(\Delta/\Delta)i}$ bone marrow at the indicated time post-poly(I/C) injection. Bar graphs indicate the total cell number (mean ± SD; n = 3) per four long bones or per spleen for each of the indicated populations in control *junB*$^{f/f}$ and poly(I/C)-injected *junB*$^{(\Delta/\Delta)i}$ mice.

and S-G_2/M cells in control LT-HSC populations and *jun*B-deficient LT-HSC populations isolated from 6- to 9-month-old *jun*B$^{-/-}$Ubi-*jun*B mice (Figure 5A). Since the absolute numbers of LT-HSC are increased in these MPD mice, this result indicates an increase in both resting and cycling LT-HSC numbers. Consistently, proliferation analyses of single LT-HSC cultured in Terasaki plates indicated faster proliferation rates and increased cell numbers generated from a single *jun*B$^{-/-}$Ubi-*jun*B LT-HSC compared to control LT-HSC (Figure 5B). However, *jun*B-deficient and control LT-HSC gave rise with similar efficiency to the entire range of myeloid and erythroid colonies in methylcellulose CFU assays (Figure 5C), indicating that both LT-HSC populations are equivalent in their differentiation capabilities in vitro and in vivo. Interestingly, *jun*B-deficient LT-HSC showed decreased mRNA levels of the cell cycle inhibitor *p16*^{Ink4a}, a direct *jun*B-target gene (Passegué and Wagner, 2000) and a

Table 1. The Transplantable Leukemic Stem Cells for the *jun*B-Deficient MPD Reside in the LT-HSC Compartment

	Number of Donors	Number of Cells	Number of Recipients	Observation Time (Months)	MPD	Blast Crisis
*jun*B$^{-/-}$Ubi-*jun*B						
Bone marrow	5	2×10^6	16	2–12	16/16	2/16
c-Kit-depleted BM	4	5×10^6	5	up to 12	0/5	
LT-HSC	4	2,000	9	2–5	9/9	1/9
ST-HSC & MPP	4	3,000	10	up to 12	0/10	
CMP	3	5,000	7	up to 5	0/7	
GMP	3	10,000	8	up to 5	0/8	
CMP, GMP, and MEP	2	5×10^5	4	up to 12	0/4	
Spleen	2	5×10^6	6	up to 12	5/6	
*jun*B$^{f/f}$MORE-*Cre* (*jun*B$^{\Delta/\Delta}$)						
Bone marrow	3	2×10^6	5	6–12	5/5	0/5
LT-HSC	3	2,000	8	5–12	8/8	1/8
CMP, GMP, and MEP	3	5×10^5	5	up to 12	0/5	
*jun*B$^{f/f}$Mx-*Cre* (*jun*B$^{(\Delta/\Delta)i}$)						
Bone marrow	2	2×10^6	6	6–12	6/6	0/6
LT-HSC	2	2,000	6	8–12	6/6	0/6
CMP, GMP, and MEP	2	5×10^5	4	up to 12	0/4	

Sublethally irradiated *RAG2*$^{-/-}$-Ly5.2 recipient mice were injected with the indicated numbers of donor bone marrow cells, spleen cells, or purified stem and/or progenitor populations isolated from 6- to 9-month-old *jun*B$^{-/-}$Ubi-*jun*B-Ly5.1 mice, 3-month-old *jun*B$^{f/f}$MORE-*Cre* (*jun*B$^{\Delta/\Delta}$)-Ly5.1 mice, or *jun*B$^{f/f}$Mx-*Cre* (*jun*B$^{(\Delta/\Delta)i}$)-Ly5.1 mice 4 months after poly(I/C) injection. Recipient mice were monitored monthly by flow cytometric analysis of peripheral blood and scored positive for MPD when neutrophil counts were above 50%. Spleen and bone marrow cells from the diseased recipient mice were further analyzed by flow cytometry and histology to confirm the MPD diagnosis and to determine the occurrence of blast crisis.

key regulator of stem cell proliferation/senescence (Park et al., 2003), and increased expression of the antiapoptotic proteins *bcl*$_2$ and *bcl*$_{x(L)}$, two critical regulators of stem cell death (Domen, 2000) (Figures 5D and 5E). Conversely, cell cycle analysis of Ly5.2$^+$/GFP$^+$-transduced *jun*B(L)-expressing LT-HSC, isolated from recipient mice 9 weeks after transplantation, revealed a significant decrease in the numbers of cycling cells compared to Co(L)-expressing LT-HSC (Figure 5F); and proliferation analysis of single Ly5.2$^+$/GFP$^+$-transduced *jun*B(L)-expressing LT-HSC in Terasaki plates also indicated a reduction in the numbers of cells generated from a single stem cell (Figure 5G). Most importantly, analysis by qRT-PCR indicated a massive increase in the levels of *p16*^{Ink4a} expressed in Ly5.2$^+$/GFP$^+$ *junB*(L)-transduced HSC-derived cells as well as some decrease in the levels of *bcl*$_2$ and *bcl*$_{x(L)}$ expressed (Figure 5H). Taken together, these findings underscore the key biological function of JunB in regulating homeostasis of the stem cell compartment (Figure 6). The expanded population of LT-HSC found in *jun*B-deficient MPD mice could arise from deregulated self-renewing replication, which occurs without impaired differentiation, and/or could be mediated through blockade of apoptosis and/or senescence, while the stem cell loss caused by increased JunB levels could be due to decreased proliferation, increased senescence, and/or increased apoptosis.

Discussion

In the present study, we demonstrate that the transcription factor JunB plays a key biological role in controlling homeostasis of the hematopoietic stem cell compartment (Figure 6). We found that raising JunB levels in LT-HSC through lentiviral transduction leads to stem cell loss, while inactivating JunB expression in LT-HSC inevitably causes a leukemogenic stem cell expansion leading to MPD development. MPD was observed in every mouse model in which we could establish conditions for LT-HSC deletion of *jun*B, either in a stochastic manner (*jun*B$^{-/-}$Ubi-*jun*B model) or in a direct manner (*jun*B$^{f/f}$More-*Cre* and *jun*B$^{f/f}$Mx-*Cre* models). Both *jun*B deletion and *jun*B overexpression deregulate cellular mechanisms, such as proliferation/senescence and apoptosis, that are critical for maintenance of the stem cell compartment. JunB effects are mediated, at least in part, via regulation of the expression of key effectors genes, like *p16*^{Ink4a}, *bcl*$_2$, and *bcl*$_{x(L)}$, which also have been shown to be important in mediating JunB effects during myelopoiesis (Passegué et al., 2001). Recently, *Bmi*-1, a negative regulator of *p16*^{Ink4a}, has been shown to be critical for the self-renewal capability of normal hematopoietic stem cells (Park et al., 2003) and myeloid leukemia cells (Lessard and Sauvageau, 2003), as well as of central nervous system (CNS) and peripheral nervous system (PNS) stem cells (Molofsky et al., 2003). Deregulation of other molecular pathways perhaps involved in controlling stem cell self-renewal (Reya et al., 2001), inhibition of programmed cell death (Traver et al., 1998), or conservation of telomeres (Allsopp and Weissman, 2002) are also likely to contribute to the leukemic fate of the *jun*B-deficient LT-HSC and are currently being investigated.

Although targeted inactivation of JunB in stem cells leads to a massive expansion of the LT-HSC population, normal numbers of ST-HSC, MPP, CLP, and CMP were derived from *jun*B-deficient LT-HSC, indicating that JunB does not control the population size of these progenitor compartments. Other genes and/or environmental influences, which are still unknown, are therefore likely to independently regulate the numbers of these hematopoietic subsets. In contrast, JunB expression is critical for homeostasis of the granulocytic lineage since *jun*B-deficient LT-HSC produce vastly increased num-

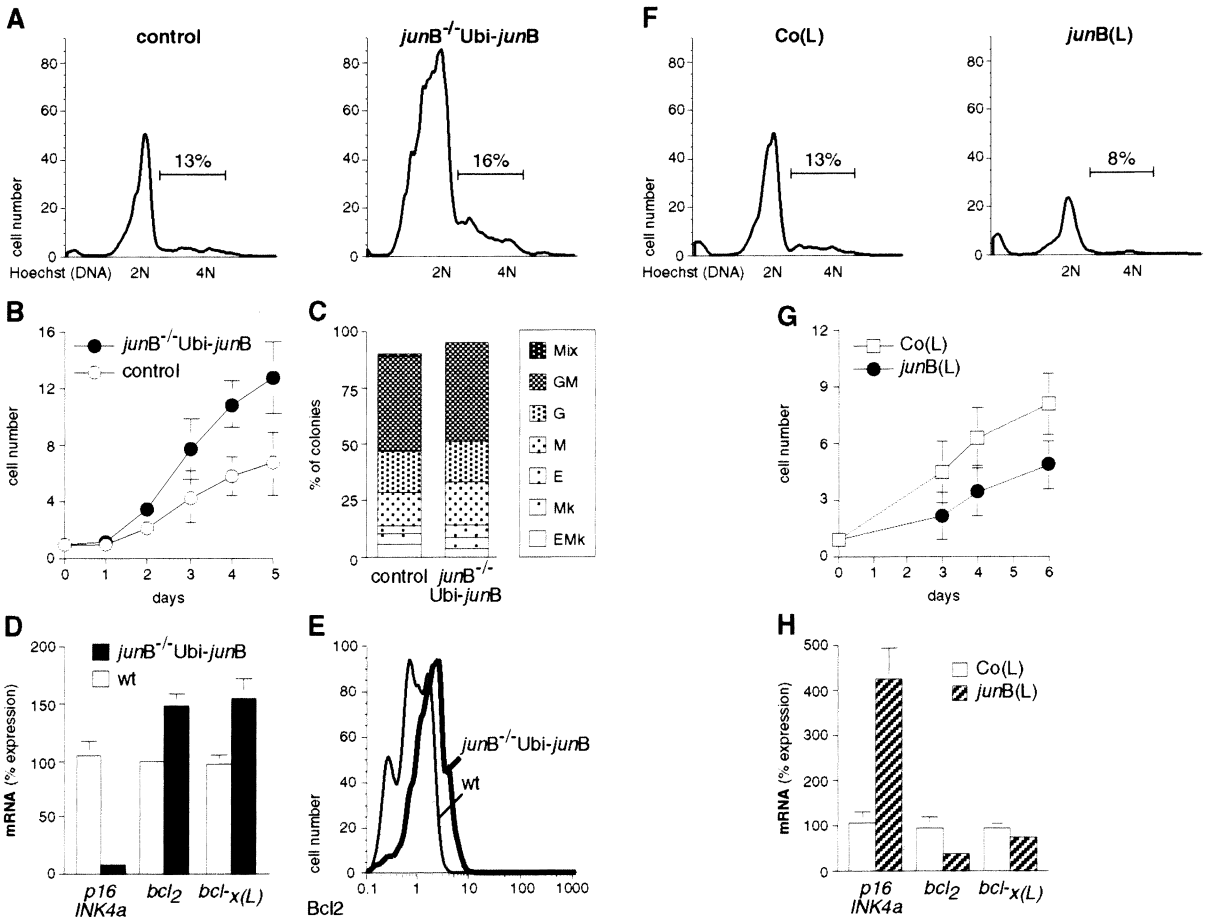

Figure 5. JunB Alters the Homeostasis of the Stem Cell Compartment due to Changes in Proliferation and Apoptosis

(A–E) Analysis of LT-HSC purified from 6- to 9-month-old control (*junB*$^{+/+}$ or *junB*$^{+/-}$ with or without the Ubi-*junB* transgene) and *junB*$^{-/-}$Ubi-*junB* mice. (A) Hoechst-33342 staining for DNA content. The percent of cells in S-G2/M phase of the cell cycle (with ≥2N DNA content) is indicated. (B) Analysis of the proliferation rate of single LT-HSC. Data are plotted as the total number (mean ± SD) of cells per Terasaki well over a 5 day period in culture. (C) Methylcellulose colony-forming units (CFU) assays. Colony types include mix (Mix), granulocyte/macrophage (GM), granulocyte (G), macrophage (M), erythroid (E), megakaryocyte (Mk), and erythroid/megakaryocyte (EMk). Granulocyte-containing colonies derived from *junB*$^{-/-}$Ubi-*junB* LT-HSC are always larger in size than colonies derived from control LT-HSC (not shown). (D) QRT-PCR analysis of $p16^{Ink4a}$, bcl_2, and $bcl_{x(L)}$ mRNA levels. Results (mean ± SD; n = 3) have been standardized for β-actin levels and are expressed as percentages of the levels detected in wild-type (wt) LT-HSC (set at 100%). (E) Intracellular staining for mouse Bcl_2. Data are plotted as histograms of fluorescence intensity.

(F–G) Analysis of (Ly5.2$^+$/GFP$^+$) LT-HSC purified from mice transplanted with Co(L)- or *junB*(L)-transduced HSC at 9 months post-transplantation. (F) Hoechst-33342 staining for DNA content. (G) Analysis of the proliferation rate of single LT-HSC.

(H) QRT-PCR analysis of $p16^{Ink4a}$, bcl_2, and $bcl_{x(L)}$ mRNA levels in (Ly5.2$^+$/GFP$^+$) spleen cells purified from mice transplanted with Co(L)- or *junB*(L)-transduced HSC at 9 months post-transplantation. Results (mean ± SD; n = 3) have been standardized for β-actin levels and are expressed as percentages of the levels detected in Co(L)-transduced cells (set at 100%).

bers of GMP and of mature granulocytes as already reported (Passegué et al., 2001). Interestingly, enforced expression of JunB in LT-HSC leads to a dramatic decline in the numbers of mature cells belonging to all the hematopoietic lineages, while *junB* inactivation leads to a specific increase in LT-HSC and GMP/granulocyte populations. Since *junB*-overexpressing HSC are lost, the effects on mature populations may be secondary to that loss, although we cannot yet exclude a more promiscuous effect of *junB* overexpression that could involve additional regulatory pathways distinct from the ones affected in *junB*-deficient LT-HSC. Most importantly, targeted inactivation of *junB* in mouse-committed myelomonocytic cells only modestly affects the homeostasis of the granulocytic lineage and never leads to MPD development, clearly indicating that the target cell for JunB inactivation is critical for the leukemogenic process. In fact, transplantation experiments indicate that LT-HSC, but not GMP or other multipotent or oligopotent progenitor population, are the only cell population capable of propagating the *junB*-deficient MPD in recipient mice. Taken together, these results demonstrate that the LT-HSC population contains the LSC for the *junB*-deficient MPD and identify this disease as a hematopoietic stem cell leukemia.

Perhaps the most common MPD in man is the chronic phase of CML (Sawyers, 1999). Acquisition of the t(9;22) Bcr-Abl translocation is an early and almost constant

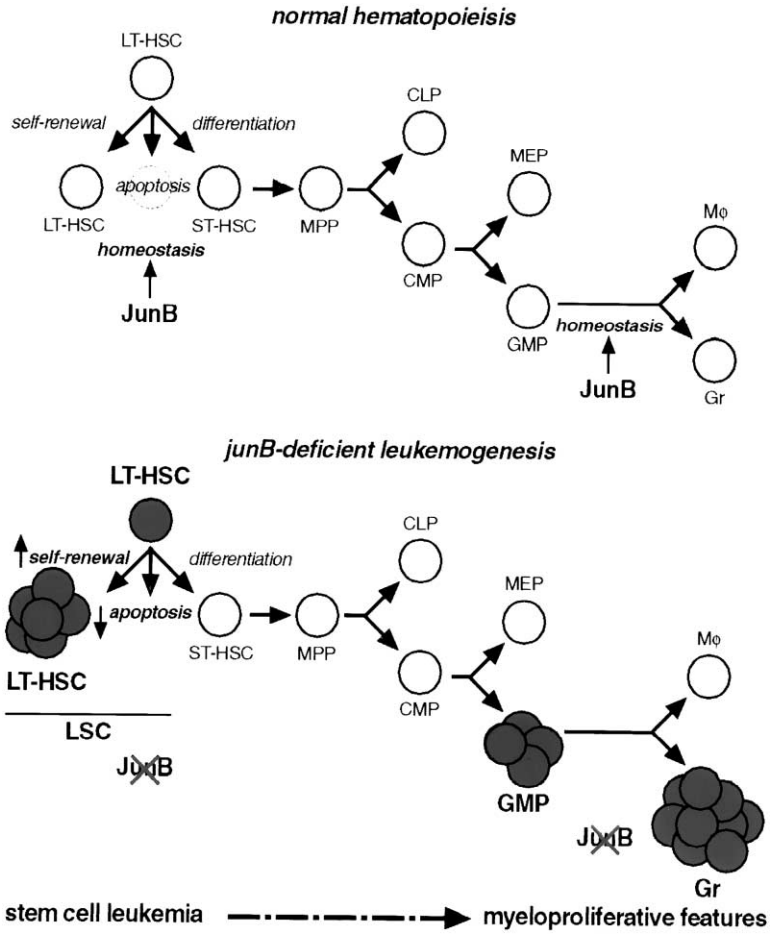

Figure 6. Proposed Model for the Role of JunB during Normal and Leukemic Hematopoiesis

During normal hematopoiesis, JunB regulates the homeostasis of the stem cell compartment by controlling the balance between self-renewal replication and apoptosis. In *jun*B-deficient mice, the absence of JunB leads to increased numbers of LT-HSC, due, at least in part, to increased proliferation and/or blockade of apoptosis, while the numbers of differentiating ST-HSC, MPP, CLP, and CMP remain normal. JunB also controls the homeostasis of the granulocytic lineage leading to a vast expansion of GMP and mature granulocytes in mice harboring stem cell inactivation of *jun*B. The expanded population of LT-HSC is the LSC of the *jun*B-deficient MPD, e.g., the only population capable of transplanting the disease to recipient mice, while the expanded GMP and granulocyte populations provide the myeloproliferative features of this stem cell leukemia.

event in human chronic phase CML. The activity of the Bcr-Abl fusion protein is central in the development of CML, but it is now clear that other transformation events are also required for its leukemic progression. The Bcr-Abl translocation can be found in normal human hematopoietic cells in the absence of leukemic transformation (Bose et al., 1998; Matioli, 2002), suggesting the existence and likely importance of additional mutations and/or epigenetic changes that could be required alone or in conjunction with Bcr-Abl for CML pathogenesis (Fialkow et al., 1981; Clarkson et al., 2003; Feldman et al., 2003). Transgenic mice overexpressing the Bcr-Abl oncogene in hematopoietic lineages also have requirements for leukemic evolution. In fact, Bcl_2-mediated inhibition of apoptosis in mice (Jaiswal et al., 2003) and recently β-catenin-driven self-renewal in humans (Jamieson et al., 2004), have been implicated as synergistic events for CML progression to its final blast crisis stage. Remarkably, *jun*B expression is inactivated in peripheral blood cells of Bcr-Abl-positive CML patients (Bruchova et al., 2002; Yang et al., 2003), mainly due to, or sustained by, hypermethylation silencing of the *jun*B promoter (Yang et al., 2003). Furthermore, the demethylating agent Decitabine, which shows encouraging anti-CML activity and promising results for the treatment of Imatinib Mesylate-resistant (Gleevec, formally STI571) patients (Kantarjian et al., 2003), leads to partial reactivation of human *jun*B expression that had previously been silenced by promoter hypermethylation (Yang et al., 2003). JunB is also regulated by the homeoprotein HoxA9 and consistent downregulation of *jun*B expression is observed in AML patients with high HoxA9 expression (Dorsam et al., 2003). Together, these findings suggest that *jun*B inactivation could be a general mechanism involved in myeloid leukemias and a contributing factor for some of the human CML pathologies that show granulocytocis and myeloid blast crisis.

Here, we clearly demonstrate that *jun*B inactivation must occur in LT-HSC, and not at later stages of myelopoiesis, to induce MPD development. In contrast, restricted expression of Bcr-Abl in mouse-committed myelomonocytic cells can lead to CML development without stem cell involvement (Jaiswal et al., 2003). Although the hMRP8-*Bcr-Abl* model may not recreate the full spectrum of human CML diseases, particularly the lymphoid crisis component, it suggests that expression of Bcr-Abl may be required only at the committed myelomonocytic stage to cause the disease, although the translocation would have to be present (through not necessarily expressed) in LT-HSC, as these are the only self-renewing cells in the hematopoietic system. Together, these results suggest a progression in the CML leukemogenesis process that could eventually apply to some human pathologies. Hence, stem cell inactivation of *jun*B could precede or follow acquisition of Bcr-Abl expression by the stem cells, or by more committed

myeloid progenitor populations, and cooperate with Bcr-Abl for the genesis and/or progression of chronic phase CML. This role for *jun*B is currently under investigation and the *jun*B-deficient MPD mice may prove to be valuable mouse models to study Bcr-Abl-independent mechanisms that may function alone or in cooperation with Bcr-Abl in the genesis and/or progression of CML. Studying the relationship between Bcr-Abl signaling and *jun*B regulation at both the HSC and the GMP level also may provide insight as to why granulocytosis predominates in human CML.

The results presented here provide the first experimental demonstration of the hematopoietic stem cell leukemia nature of an MPD similar to human chronic phase CML. They nicely corroborate the less direct evidence that the chronic phase of human CML is a clonal expansion of multiple hematopoietic lineages and therefore derives from HSC or other multipotent cells (Fialkow et al., 1977; Li et al., 1999). The identification of the LSC for the *jun*B-deficient MPD lends further support to the notion that leukemias and cancers may be sustained by rare LSC or cancer stem cells (Reya et al., 2001; Passegué et al., 2003) that could either derive from the stem cell of the tissue of origin, as shown here, or from more restricted progenitors that have reacquired the stem cell capability for self-renewal, as we have recently shown for MLL-ENL-induced mouse AML (Cozzio et al., 2003), in human myeloid blast crisis CML (Jamieson et al., 2004) and in other human AML (Miyamoto et al., 2000). Insofar as the only self-renewing cell in the myeloid lineage is the LT-HSC, we expect that only clones of LT-HSC can accumulate all the mutations and/or epigenetic changes involved in the progression to leukemia, including several independent events to inhibit programmed cell death (Traver et al., 1998), to inhibit differentiation (Tenen, 2003) and to enforce self-renewal (Reya et al., 2001; Jamieson et al., 2004). Future investigations of the *jun*B-deficient LT-HSC should therefore provide a better molecular understanding of LSC pathogenesis and may lead to new insights into some features of human MPD including CML.

Experimental Procedures

Mouse

The congenic mouse strains C57BL/6-Ly5.1 or Ly5.2 and the *RAG2*$^{-/-}$-Ly5.2 mice were used as described (Kondo et al., 1997). *Jun*B$^{-/-}$Ubi-*jun*B (Schorpp-Kistner et al., 1999), *jun*B$^{f/f}$ (Kenner et al., 2004), MORE-*Cre* (Tallquist and Soriano, 2000), and Mx-*Cre* (Kühn et al., 1995) mice were generated as described. The MRP8-*Cre*-ires/GFP construct was generated by inserting a *Cre*-ires/GFP cassette into the unique BglII site of the human MRP8 expression vector (Lagasse and Weissman, 1994) and two founder transgenic lines were obtained after DNA microinjection into fertilized F1 (C57BL/6 × C3H) eggs. All the mice were backcrossed between two to seven times to the C57BL/6 background before being used for the experiments. To induce Mx-*Cre*-mediated deletion of *jun*B during adult hematopoiesis, 4-week-old *jun*B$^{f/f}$Mx-*Cre* mice were injected four times at 2-day intervals with 250 μg poly(I/C) in 200 μl PBS. All mice were maintained in Stanford University's Research Animal Facility in accordance with Stanford University guidelines. The classification of the nonlymphoid hematopoietic neoplasm described in this study was performed according to the guidelines edited by the hematopathology subcommittee of the mouse models of human cancers consortium (Kogan et al., 2002). Indolent granulocytic expansion corresponds to an increase by ≤2-fold in the total number of granulocyte in the bone marrow and no extramedullar hematopoiesis. Myeloproliferative disease (MPD) corresponds to an increase by ≥2-fold in the total number of granulocytes in the bone marrow and to an increase in the relative frequency of granulocytes by ≥20% in the spleen and by ≥50% in the blood, extramedullar hematopoiesis, and transplantability of the disease. Overt myeloid leukemia corresponds to all the previous plus anemia and ≥20% blast cells.

Flow Cytometry

Cell staining and enrichment procedures for cell sorting were performed as described (Kondo et al., 1997; Akashi et al., 1999; Christensen and Weissman, 2001). Cells were finally resuspended in Hanks Buffered Salt Solution (HBSS) with 2% heat-inactivated fetal-calf serum (staining medium) and 1 μg/ml propidium iodide (PI) and analyzed or sorted on a modified 488 nm argon and 599 nm dye dual laser FACS Vantage (Becton Dickinson Immunocytometry System). Dead cells were gated out by high PI staining and forward light scatter. For proliferation analysis of a single stem cell, one LT-HSC was clone-sorted per well of a Terasaki plate in 10 μl of Iscove's Modified Dulbecco's Media (IMDM) containing 5% FCS, 50 mM 2-βmercaptoethanol, SCF (20 ng/ml), Flt3L (20 ng/ml), and IL-11 (10 ng/ml) and incubated at 37°C for the indicated duration. The numbers of cells per well were visually determined using an inverted microscope. For Hoechst analysis, c-Kit-enriched bone marrow cells were preincubated for 45 min at 37°C in staining medium containing 1 g/ml glucose, 20 μg/ml Hoechst-33342 (Molecular Probes), and 50 μg/ml Verapamil before the final staining step, also performed in the presence of 50 μg/ml Verapamil. Intracellular $mBcl_2$ staining was performed as described (Domen et al., 1998).

Cell Transplantation

Unfractionated bone marrow and spleen cells and purified stem and progenitor populations were obtained from 6- to 9-month-old *jun*B$^{-/-}$Ubi-*jun*B-Ly5.1 mice, 3-month-old *jun*B$^{f/f}$MORE-*Cre* (*jun*B$^{\Delta/\Delta}$)-Ly5.1 mice, or *jun*B$^{f/f}$Mx-*Cre* (*jun*B$^{(\Delta/\Delta)I}$)-Ly5.1 mice 4 months after poly(I/C) injection and transplanted via retro-orbital injection into sublethally irradiated (450 rad) *RAG2*$^{-/-}$-Ly5.2 recipient mice. Peripheral blood was obtained from the tail vein of each mouse and analyzed by flow cytometry. Donor-derived cells were distinguished from host cells by the expression of different Ly5 antigens (Ly5.1 versus Ly5.2).

HSC Lentiviral Transduction and Transplantation

*Jun*B cDNA was cloned upstream of an ires/eGFP sequence into a self-inactivating lentiviral vector plasmid and viral stocks were produced by triple transfection of 293T cells along with lentiviral gag-pol and vesicular stomatitis virus G glycoprotein constructs. Lentivirus-containing supernatant medium was collected for 2 consecutive days and concentrated by ultracentrifugation. HSC were purified from C57BL/6-Ly5.2 mice and cultured in 200 μl in 96-well plates with concentrated lentiviral stocks (1:50 to 1:100 dilution) in Iscove's Modified Dulbecco's Media (IMDM) containing 5% FCS, 50 μM 2-mercaptoethanol, SCF (20 ng/ml), Flt3L (20 ng/ml), and IL-11 (10 ng/ml) for 12–16 hr at 37°C. Transduced HSC were mixed with a radioprotective dose of 2.5×10^5 congenic Sca-1-depleted C57BL/6-Ly5.1 helper bone marrow cells and transplanted via retro-orbital injection into lethally irradiated (960 rad) congenic C57BL/6-Ly5.1 recipients.

Methylcellulose CFU Assays

To support the formation of myeloid colonies, purified LT-HSC (100 cells) were cultured in Iscove's Modified Dulbecco's Media (IMDM)-based methylcellulose media (Methocult M3100, StemCell Technologies) supplemented as described (Akashi et al., 1999).

Quantitative RT-PCR Analysis

Total RNA was isolated using Trizol reagent (Invitrogen) from purified HSC (2,000 to 5,000 cells), progenitors (10,000 to 30,000 cells), or mature cell populations (30,000 to 100,000 cells), digested with DNase I to remove DNA contamination and used for reverse-transcription according to the manufacturer's instructions (SuperScript II™ kit, Invitrogen). For qRT-PCR analysis, primer sequences were

designed using Primer Express software (Applied Biosystems) and are available upon request. All reactions were performed in an ABI-7000 sequence detection system using SYBR Green PCR Core reagents according to the manufacturer's instructions (Applied Biosystems). PCR amplification was performed in a 12 μl final volume containing 1X SYBR Green PCR buffer, 2 mM magnesium chloride, 0.5 mM dNTP mix with dUTP, 8 ng of each primer, 0.1 U AmpErase UNG, 0.25 U AmpliTaq Gold, and 2 μl of DNA or cDNA templates using 50°C for 2 min and 95°C for 10 min followed by 45 cycles at 95°C for 15 s and 60°C for 1 min. For each sample, expression of the β-actin gene was used to normalize the amount of the investigated transcript.

Acknowledgments

We are grateful to L. Krenner for providing us with the *jun*B$^{\Delta/\Delta}$ mice. We thank L. Ailles, T. Serwold, and A. Wagers for critical reading of the manuscript, L. Jerabek for lab management, M. Muijtjens and S. Smith for DNA microinjection, O. Zilian for the Mx-*Cre* mice, and L. Hidalgo and B. Lavarro for animal care. E.P. was supported by an EMBO long-term fellowship and is currently a fellow of the Jose Carreras International Leukemia Foundation. This work was supported by the NIH (CA55209; CA86017) and a De Villier Award from the Leukemia and Lymphoma Society to I.L.W.

Received: June 28, 2004
Revised: August 26, 2004
Accepted: September 7, 2004
Published: October 28, 2004

References

Akashi, K., Traver, D., Miyamoto, T., and Weissman, I.L. (1999). A clonogenic common myeloid progenitor that give rise to all myeloid lineages. Nature *404*, 193–197.

Allsopp, R.C., and Weissman, I.L. (2002). Replicative senescence of hematopoietic stem cells during serial transplantation: does telomere shortening play a role? Oncogene *21*, 3270–3273.

Antonchuk, J., Sauvageau, G., and Humphries, R.K. (2002). HOXB4-induced expansion of adult hematopoietic stem cells *ex vivo*. Cell *109*, 39–45.

Bhardwaj, G., Murdoch, B., Wu, D., Baker, D.P., Williams, K.P., Chadwick, K., Ling, L.E., Karanu, F.N., and Bhatia, M. (2001). Sonic hedgehog induces the proliferation of primitive human hematopoietic cells via BMP regulation. Nat. Immunol. *2*, 172–180.

Bose, S., Deininger, M., Gora-Tybor, J., Goldman, J.M., and Melo, J.V. (1998). The presence of typical and atypical BCR-ABL fusion genes in leukocytes of normal individuals: biologic significance and implication for the assessment of minimal residual disease. Blood *92*, 3362–3367.

Bruchova, H., Borovanova, T., Klamova, H., and Brdicka, R. (2002). Gene expression profiling in chronic myeloid leukemia patients treated with hydroxyurea. Leuk. Lymphoma *43*, 1289–1295.

Christensen, J.L., and Weissman, I.L. (2001). Flk-2 is a marker in hematopoietic stem cell differentiation: a simple method to isolate long-term stem cells. Proc. Natl. Acad. Sci. USA *98*, 14541–14546.

Clarkson, B., Stife, A., Wisniewski, D., Lambek, C.L., and Liu, C. (2003). Chronic myelogenous leukemia as a paradigm of early cancer and possible curative strategies. Leukemia *17*, 1211–1262.

Cozzio, A., Passegué, E., Ayton, P.M., Karsunky, H., Cleary, M.L., and Weissman, I.L. (2003). Similar MLL-associated leukemias arising from self-renewing stem cells and short-lived myeloid progenitors. Genes Dev. *17*, 3029–3035.

Domen, J. (2000). The role of apoptosis in regulating hematopoiesis and hematopoietic stem cells. Immunol. Res. *22*, 83–94.

Domen, J., Gandy, K.L., and Weissman, I.L. (1998). Systemic overexpression of BCL-2 in the hematopoietic system protects transgenic mice from the consequences of lethal irradiation. Blood *91*, 2272–2282.

Dorsam, S.T., Ferrell, C.M., Dorsam, G.P., Derynck, M.K., Vijapurkar, U., Khodabakhsh, D., Pau, B., Bernstein, H., Haqq, C.M., Largman, C., and Lawrence, H.J. (2003). The transcriptome of the leukemogenic homeoprotein HOXA9 in human hematopoietic cells. Blood *103*, 1676–1684.

Feldman, E., Najfeld, V., Schuster, M., Roboz, G., Chadburn, A., and Silver, R.T. (2003). The emergence of Ph$^-$, trisomy-8$^+$ cells in patients with chronic myeloid leukemia treated with imatinib mesylate. Exp. Hematol. *31*, 702–707.

Fialkow, P.J., Jacobson, R.J., and Papayannopoulou, T. (1977). Chronic myelocytic leukemia: clonal origin in a stem cell common to the granulocyte, erythrocyte, platelet and monocyte/macrophage. Am. J. Med. *63*, 125–130.

Fialkow, P.J., Martin, P.J., and Najfed, V. (1981). Evidence of a multistep pathogenesis of chronic myelogenous leukemia. Blood *58*, 158–163.

Jamieson, C.H., Ailles, L.E., Dylla, S.J., Muijtjens, M., Jones, C., Zehnder, J.L., Gotlib. J., Li, K., Manz, M.G., Keating, A., Sawyers, C.L., and Weissman, I.L. (2004). Granulocyte/Macrophage progenitors in chronic myelogenous leukemia are candidate leukemic stem cells that activate the beta-catenin pathway. N. Engl. J. Med. *351*, 657–667.

Jaiswal, S., Traver, D., Miyamoto, T., Akashi, K., Lagasse, E., and Weissman, I.L. (2003). Development of murine chronic and acute myelogenous leukemia with targeted expression of BCR/ABL to myeloid progenitors. Proc. Natl. Acad. Sci. USA *100*, 10002–10007.

Kantarjian, H.M., O'Brien, S., Cortes, J., Giles, F.J., Faderl, S., Issa, J.P., Garcia-Manero, G., Rios, M.B., Shan, J., Andreeff, M., Keating, M., and Talpaz, M. (2003). Results of decitabine (5-aza-2′deoxycytidine) therapy in 130 patients with chronic myelogenous leukemia. Cancer *98*, 522–528.

Kenner, L., Hoebertz, A., Beil, T., Keon, N., Karreth, F., Eferl, R., Scheuch, H., Szremska, A., Amling, M., Schorpp-Kistner, M., Angel, P., and Wagner, E.F. (2004). Mice lacking JunB are osteopenic due to cell autonomous osteoblast and osteoclast defects. J. Cell Biol. *164*, 613–623.

Kogan, S.C., Ward, J.M., Anver, M.R., Berman, J.J., Brayton, C., Cardiff, R.D., Carter, J.S., de Coronado, S., Downing, J.R., and Fredrickson, T.N. (2002). Bethesda proposals for classification of nonlymphoid hematopoietic neoplasms in mice. Blood *100*, 238–245.

Kondo, M., Weissman, I.L., and Akashi, K. (1997). Identification of clonogenic common lymphoid progenitors in mouse bone marrow. Cell *91*, 661–672.

Kühn, R., Schwenk, F., Aguet, M., and Rajewsky, K. (1995). Inducible gene targeting in mice. Science *269*, 1427–1429.

Lagasse, E., and Weissman, I.L. (1994). bcl-2 inhibits apoptosis of neutrophils but not their engulfment by macrophages. J. Exp. Med. *179*, 1047–1052.

Lessard, J., and Sauvageau, G. (2003). Bmi-1 determines the proliferative capacity of normal and leukaemic stem cells. Nature *423*, 255–260.

Li, S., Ilaria, R.L., Jr., Million, R.P., Daley, G.Q., and Van Etten, R.A. (1999). The p190, p220, and p230 forms of the Bcr-Abl oncogene induce a similar chronic myeloid leukemia-like symdrome in mice but have different lymphoid leukemogenic activity. J. Exp. Med. *189*, 1399–1412.

Matioli, G.T. (2002). BCR-ABL insufficiency for the transformation of human stem cells into CML. Med. Hypotheses *59*, 588–589.

Miyamoto, T., Weissman, I.L., and Akashi, K. (2000). AML1/ETO-expressing nonleukemic stem cells in acute myelogenous leukemia with 8;21 chromosomal translocation. Proc. Natl. Acad. Sci. USA *97*, 7521–7526.

Molofsky, A.V., Pardal, R., Iwashita, T., Park, I.K., Clarke, M.F., and Morrison, S.J. (2003). Bmi-1 dependence distinguishes neural stem cell self-renewal from progenitor proliferation. Nature *425*, 962–967.

Morrison, S.J., Wright, D.E., and Weissman, I.L. (1997). Identification of a lineage of multipotent hematopoietic progenitors. Development *124*, 1929–1939.

Na Nakorn, T., Traver, D., Weissman, I.L., and Akashi, K. (2002). Myeloerythroid-restricted progenitors are sufficient to confer radio-

protection and provide the majority of day 8 CFU-S. J. Clin. Invest. *199*, 1579–1585.

Orkin, S.H. (2000). Diversification of hematopoietic stem cells to specific lineages. Nat. Rev. Genet. *1*, 57–64.

Park, I.-K., Qian, D., Kiel, M., Becker, M.W., Pihalja, M., Weissman, I.L., Morrison, S.J., and Clarke, M.F. (2003). Bmi-1 is required for maintenance of adult self-renewing haematopoietic stem cells. Nature *423*, 302–305.

Passegué, E., and Wagner, F. (2000). JunB suppresses cell proliferation by transcriptional activation of p16(INK4a) expression. EMBO J. *19*, 2969–2979.

Passegué, E., Jochum, W., Schorpp-Kistner, M., Möhle-Steinlein, U., and Wagner, E.F. (2001). Chronic myeloid leukemia with increased granulocyte progenitors in mice lacking JunB expression in the myeloid lineage. Cell *104*, 21–32.

Passegué, E., Jamieson, C.H.E., Ailles, L.E., and Weissman, I.L. (2003). Normal and leukemic hematopoiesis: are leukemias a stem cell disorder or a reacquisition of stem cell characteristics? Proc. Natl. Acad. Sci. USA *100* Suppl. 1, 11842–11849.

Reya, T., Morrison, S.J., Clarke, M.F., and Weissman, I.L. (2001). Stem cells, cancer, and cancer stem cells. Nature *414*, 105–111.

Reya, T., Duncan, A., Ailles, L., Domen, J., Scherer, D., Willert, K., Hintz, L., Nusse, R., and Weissman, I.L. (2003). Regulation of hematopoietic stem cell self renewal by the Wnt signaling pathway. Nature *423*, 409–414.

Sawyers, C.L. (1999). Chronic myeloid leukemia. N. Engl. J. Med. *340*, 1330–1340.

Schorpp-Kistner, M., Wang, Z.-Q., Angel, P., and Wagner, E.F. (1999). JunB is essential for mammalian placentation. EMBO J. *18*, 934–948.

Spangrude, G.J., Heimfeld, S., and Weissman, I.L. (1988). Purification and characterization of mouse hematopoietic stem cells. Science *241*, 58–62.

Tallquist, M.D., and Soriano, P. (2000). Epiblast-restricted Cre expression in MORE mice: a tool to distinguish embryonic *vs*. extra-embryonic gene function. Genesis *26*, 113–115.

Tenen, D.G. (2003). Disruption of differentiation in human cancer: AML shows the way. Nat. Rev. Cancer *3*, 89–101.

Thorsteinsdottir, U., Mamo, A., Kroon, E., Jerome, L., Bijl, J., Lawrence, H.J., Humphries, K., and Sauvageau, G. (2002). Overexpression of the myeloid leukemia-associated Hoxa9 gene in bone marrow cells induces stem cell. Blood *99*, 121–129.

Traver, D., Akashi, K., Weissman, I.L., and Lagasse, E. (1998). Mice defective in two apoptosis pathways in the myeloid lineage develop acute myeloblastic leukemia. Immunity *9*, 47–57.

Varnum-Finney, B., Xu, L., Brashem-Stein, C., Nourigat, C., Flowers, D., Bakkour, S., Pear, W.S., and Bernstein, I.D. (2000). Pluripotent, cytokine-dependent, hematopoietic stem cells are immortalized by constitutive Notch1 signaling. Nat. Med. *6*, 1278–1281.

Yang, M.Y., Liu, T.C., Chang, J.G., Lin, P.M., and Lin, S.F. (2003). JunB gene expression is inactivated by methylation in chronic myeloid leukemia. Blood *101*, 3205–3211.